15th Triennial World Congress, Barcelona, Spain

NOISE REJECTION STRATEGY FOR A LARGE SPACE STRUCTURE: THE GRANTECAN TELESCOPE

L. Acosta, M. Sigut, F. Martín[*], J.A. Méndez, G.N. Marichal and S. Torres

Dept. of Fundamental and Experimental Physics, Electronics and Systems, University of La Laguna
[(*)]Dept. of Fundamental Mathematics, University of La Laguna
Avda. Francisco Sánchez, s/n. La Laguna – CP:38204 - Tenerife (SPAIN)
Phone: +34 922 318286 – Fax: +34 922 319085 – E-mail: marta@cyc.dfis.ull.es

Abstract: In this paper, a series of results related to the decoupling of the 10m diameter Grantecan's primary mirror dynamics and its influence on the design of a controller for the mirror are presented. Firstly, an algebraic approach of the decoupling method, together with its general lines are shown. Some modifications of this procedure with respect to the way it was originally proposed with the aim of its simplification and improvement are also presented. Finally, a discussion about the design of a robust H_∞ controller for any of the SISO subsystems obtained after the decoupling and the corresponding results is carried out. *Copyright © 2002 IFAC*

Keywords: Large space structures, Multi-input/multi-output systems, Multivariable control systems, Decoupling problems, H-infinity control.

1. INTRODUCTION

Before the Keck Telescope (Mauna Kea, Hawaii) and the Gran Telescopio Canarias (GTC) (La Palma, Spain), the largest telescopes in the world had an 8m monolithic primary mirror, according to the line of many similar projects started at the end of the eighties. The aim of the GTC project was to provide a significant advance over existing 4m class telescopes. Experts in the field concluded that the entrance pupil of the GTC needed to have a diameter of at least 10m to be 1 mag more sensitive than a 4m class telescope. However, the GTC project does not simply increment the list of '8-10m class' telescopes. It combines a large collecting surface with excellent image quality and a suitably optimized observing range in both the visible and the infrared. The big size of the GTC's primary mirror has compelled to segment it into 36 hexagonal pieces. This is the reason why the active control of the mirror is necessary. The goal of the controller will be to ensure that the segments behave all the time as if they composed a monolithic mirror.

To make it possible to move the segments in the three axial degrees of freedom, each one of them is provided with three positioners. At the same time, the relative axial position of the primary mirror segments is measured using two position sensors situated in each common edge between segments. Thus, the mirror is, from the point of view of the controller, a 108 inputs-168 outputs system.

To design a centralized controller with such a high number of inputs and outputs is a complex task; while a decentralized policy does not provide a good performance since the important effect of coupling between the different segments can not be neglected. As a consequence of this, a procedure for the mirror dynamics decoupling consisting in a change of the system eigenvectors basis has been carried out. This transforms the original MIMO (multi-input/multi-output) system into a set of subsystems, many of which are SISO (single-input single-output). A robust controller has been designed for any of them with the aim of ensuring the correct alignment of the segments in presence of noise (it has been considered that it is produced by the effect of the wind over the mirror) and uncertainties in the system model (Hayakawa, 1999; Huang, 1998; Skogestad, 1998).

2. MIRROR'S DYNAMICS MODELING

Three are the main elements that compose the GTC's primary mirror. They are:

- The structure or cell, which supports each of the segments together with their active and passive support systems. Its dynamics is

characterized by the 30 dominant modes, being the most important one in 17Hz.
- The segments, modeled as a second order system with a 28Hz natural frequency.
- The positioners or actuators, characterized by a 5ms of delay and a 60Hz natural frequency.

The whole system dynamics is described by the following equations:

$$\begin{cases} \dot{\mathbf{X}}(708\times 1) = \mathbf{A}(708\times 708) * \mathbf{X} + \mathbf{B}(708\times 108) * \mathbf{U}(108\times 1) + \mathbf{P} \\ \mathbf{S}(168\times 1) = \mathbf{C}(168\times 708) * \mathbf{X} \end{cases}$$

where:

- **X** is the states vector whose components are:
  a: dominant oscillation modes of the cell (30).
  $\dot{a}$: time derivatives of these modes (30).
  x_e: distances from the segments to the cell (108).
  $m_s \dot{x}_e$: segments' momentum (108).
  $r1$, $r2$: two states associated with the time delay for each positioner (2×108).
  q, $\dot{q}$: two states associated with the positioners' dynamics (2×108).
- **A** and **B** determine the system dynamics and include terms such as:
  The cell modal displacements.
  The angular modal frequencies of the cell.
  The damping factors corresponding to the cell modes.
  The segments' base stiffness and damping factors.
  The mass associated with one of the supports of the segment with the cell.
  The positioners' natural frequency.
  The positioners' damping factor and time delay.
- **U** are the signals sent to the positioners to move the segments.
- **S** are the measurements made by the sensors.
- **P** is the vector of disturbances caused by the wind.
- **C** contains the geometric relationship between the sensors' signals and the positioners' relative positions.

3. DECOUPLING OF THE MIRROR'S DYNAMICS

From the point of view of the decoupling process, only the set cell+segments has to be considered. The positioners dynamics is already decoupled and to include it only contributes to increase the plant dimension. In figure 1, the open-loop system blocks diagram is shown:

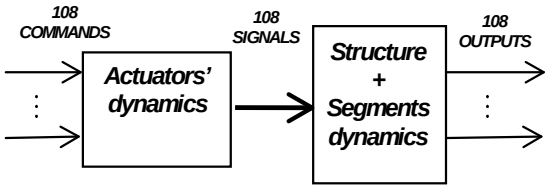

Fig. 1. Blocks diagram corresponding to the open-loop system .

The first $2N$ eigenvalues of the structure and segments states matrix correspond to the N modes used for the cell dynamic characterization, while the following correspond to the positioners considered. The value of the latter would be all equal, called 'nominal eigenvalue', if it were not for the coupling elements between the cell and the segments.

In the most general case, working with N modes for the cell and P positioners, being $P>2N$, our purpose is to demonstrate two things:

- There are P-N eigenvalues corresponding to the positioners whose value is the 'nominal' one.
- The vectorial subspace composed of the eigenvectors corresponding to the cell and the positioners coupled with it is orthogonal to the subspace composed of the non-coupled positioners.

The demonstration of these two items will be carried out in the complex domain, which is the case we are interested in.

3.1 Demonstration in the complex domain.

Consider the square matrix of complex numbers shown at the top of the next page, where $\mathbf{m}_i, i = 1,2,\cdots 8N$ is a row matrix of P real elements that is linear combination of the following real row matrices:

$$\mathbf{t}_1 = (t_{1,2N+1}, t_{1,2N+2}, \cdots t_{1,2N+2P})$$
$$\mathbf{t}_2 = (t_{2,2N+1}, t_{2,2N+2}, \cdots t_{2,2N+2P})$$
$$\vdots$$
$$\mathbf{t}_N = (t_{N,2N+1}, t_{N,2N+2}, \cdots t_{N,2N+2P})$$

and $\mathbf{m}_j^{\ t}$ denotes the traspose of the $\mathbf{m}_j$ row matrix. In addition to this, $\lambda_1, \cdots \lambda_N, \lambda_A$ are complex numbers, $\overline{\lambda_k}$ denotes the complex conjugated of λ_k and $\lambda_A^{\ l}, l = 1, \cdots P$ represents each one of the P λ_A eigenvalues.

Consider now the $E_\lambda^{\ C} \in C^{2N+2P}$ (the $2N$+$2P$ dimensional complex numbers set) vectorial subspace, being $\lambda \in C$, composed of the $\mathbf{v} = (v_1, \cdots v_{2N+2P})$ vectors complying with:

$$(\mathbf{A} - \lambda \cdot \mathbf{I}_{2N+2P}) \begin{pmatrix} v_1 \\ \vdots \\ v_{2N+2P} \end{pmatrix} = \begin{pmatrix} 0 \\ \vdots \\ 0 \end{pmatrix}$$

The $E_\lambda^{\ F}$ subspace is composed of the $\mathbf{v} = (v_1, \cdots v_{2N+2P})$ vectors satisfying that:

$$\begin{pmatrix} v_1 & \cdots & v_{2N+2P} \end{pmatrix} (\mathbf{A} - \lambda \cdot \mathbf{I}_{2N+2P}) = \begin{pmatrix} 0 & \cdots & 0 \end{pmatrix}$$

$$\mathbf{A}=\begin{pmatrix}
\lambda_1 & 0 & 0 & 0 & 0 & 0 \\
0 & \ddots & 0 & 0 & 0 & 0 \\
0 & 0 & \lambda_N & 0 & 0 & 0 \\
0 & 0 & 0 & \overline{\lambda}_1 & 0 & 0 \\
0 & 0 & 0 & 0 & \ddots & 0 \\
0 & 0 & 0 & 0 & 0 & \overline{\lambda}_N \\
\mathbf{m}_{4N+1}{}^t & \cdots & \mathbf{m}_{5N}{}^t & \mathbf{m}_{5N+1}{}^t & \cdots & \mathbf{m}_{6N}{}^t \\
\mathbf{m}_{6N+1}{}^t & \cdots & \mathbf{m}_{7N}{}^t & \mathbf{m}_{7N+1}{}^t & \cdots & \mathbf{m}_{8N}{}^t
\end{pmatrix}$$

$$\begin{pmatrix}
\mathbf{m}_1 & & \mathbf{m}_{2N+1} & & \\
\vdots & & \vdots & & \\
\mathbf{m}_N & & \mathbf{m}_{3N} & & \\
\mathbf{m}_{N+1} & & \mathbf{m}_{3N+1} & & \\
\vdots & & \vdots & & \\
\mathbf{m}_{2N} & & \mathbf{m}_{4N} & &
\end{pmatrix}$$

$$\begin{pmatrix}
\lambda_A{}^1 & 0 & 0 & 0 & 0 & 0 \\
0 & \ddots & 0 & 0 & 0 & 0 \\
0 & 0 & \lambda_A{}^P & 0 & 0 & 0 \\
0 & 0 & 0 & \overline{\lambda}_A{}^1 & 0 & 0 \\
0 & 0 & 0 & 0 & \ddots & 0 \\
0 & 0 & 0 & 0 & 0 & \overline{\lambda}_A{}^P
\end{pmatrix}$$

When there exists a subspace, W, of a complex vectorial subspace, it can be considered the $\overline{W}$ subspace composed of the complex conjugated vectors to the ones of W. In general, $\overline{W}$ does not coincide with W.

Consider now the W_{λ_A} subspace composed of the $\mathbf{v}=(v_1,\cdots v_{2N+2P})$ vectors verifying that:

$$v_1=0;\cdots v_{2N}=0;v_{2N+P+1}=0;\cdots v_{2N+2P}=0;$$

$$;\mathbf{t}_1\cdot\begin{pmatrix}v_{2N+1}\\v_{2N+2}\\\vdots\\v_{2N+P}\end{pmatrix}=0;\cdots\mathbf{t}_N\cdot\begin{pmatrix}v_{2N+1}\\v_{2N+2}\\\vdots\\v_{2N+P}\end{pmatrix}=0$$

Notice that $\overline{W}_{\lambda_A}=W_{\lambda_A}$. As a consequence of this, we have that:

$$W_{\lambda_A}\subseteq E_{\lambda_A}{}^C\cap E_{\lambda_A}{}^F\cap\overline{E}_{\lambda_A}{}^C\cap\overline{E}_{\lambda_A}{}^F.$$

Moreover:

$$P-N=2N+2P-(3N+P)\le\dim_C(W_{\lambda_A})\le$$

$$\le 2N+2P-(2N+P)=P \text{ and, consequently:}$$

$$\dim_C(E_{\lambda_A}{}^C\cap E_{\lambda_A}{}^F\cap\overline{E}_{\lambda_A}{}^C\cap\overline{E}_{\lambda_A}{}^F)\ge P-N$$

Lemma 1.- λ_A is an eigenvalue of **A** and $\dim_C(E_{\lambda_A}{}^C\cap E_{\lambda_A}{}^F\cap\overline{E}_{\lambda_A}{}^C\cap\overline{E}_{\lambda_A}{}^F)\ge P-N$.

Proposition 1.- If λ is an eigenvalue of **A**, being $\lambda\neq\lambda_A$, then:

i) The vectors of $E_\lambda{}^C$ are hermitian orthogonal to the vectors of $E_{\lambda_A}{}^C\cap\overline{E}_{\lambda_A}{}^F$.

ii) The vectors of $E_\lambda{}^F$ are hermitian orthogonal to the vectors of $E_{\lambda_A}{}^F\cap\overline{E}_{\lambda_A}{}^C$.

Proof:

i) Be $\mathbf{v}=(v_1\ \cdots\ v_{2N+2P})\in E_\lambda{}^C$ and $\mathbf{w}=(w_1\ \cdots\ w_{2N+2P})\in E_{\lambda_A}{}^C\cap\overline{E}_{\lambda_A}{}^F$.

Then, the hermitian scalar product of the **v** and **w** vectors can be written as:

$$<\mathbf{v},\mathbf{w}>=\mathbf{v}\cdot\overline{\mathbf{w}}^t$$

and:

$$\lambda\cdot<\mathbf{v},\mathbf{w}>=\lambda\cdot(v_1\ \cdots\ v_{2N+2P})\cdot\begin{pmatrix}\overline{w}_1\\\vdots\\\overline{w}_{2N+2P}\end{pmatrix}=$$

$$=(\overline{w}_1\ \cdots\ \overline{w}_{2N+2P})\cdot\lambda\cdot\begin{pmatrix}v_1\\\vdots\\v_{2N+2P}\end{pmatrix}=$$

$$=(\overline{w}_1\ \cdots\ \overline{w}_{2N+2P})\cdot\mathbf{A}\cdot\begin{pmatrix}v_1\\\vdots\\v_{2N+2P}\end{pmatrix}=$$

$$=\lambda_A\cdot(\overline{w}_1\ \cdots\ \overline{w}_{2N+2P})\cdot\begin{pmatrix}v_1\\\vdots\\v_{2N+2P}\end{pmatrix}=\lambda_A\cdot<\mathbf{v},\mathbf{w}>$$

Consequently:

$(\lambda-\lambda_A)\cdot<\mathbf{v},\mathbf{w}>=0\Rightarrow<\mathbf{v},\mathbf{w}>=0$, since $\lambda\neq\lambda_A$.

ii) If $\mathbf{v}=(v_1\ \cdots\ v_{2N+2P})\in E_\lambda{}^F$ and $\mathbf{w}=(w_1\ \cdots\ w_{2N+2P})\in E_{\lambda_A}{}^F\cap\overline{E}_{\lambda_A}{}^C$:

$$\lambda\cdot<\mathbf{v},\mathbf{w}>=\lambda\cdot(v_1\ \cdots\ v_{2N+2P})\cdot\begin{pmatrix}\overline{w}_1\\\vdots\\\overline{w}_{2N+2P}\end{pmatrix}=$$

$$=(v_1\ \cdots\ v_{2N+2P})\cdot\mathbf{A}\cdot\begin{pmatrix}\overline{w}_1\\\vdots\\\overline{w}_{2N+2P}\end{pmatrix}=$$

$$=(v_1\ \cdots\ v_{2N+2P})\cdot\lambda_A\cdot\begin{pmatrix}\overline{w}_1\\\vdots\\\overline{w}_{2N+2P}\end{pmatrix}=\lambda_A\cdot<\mathbf{v},\mathbf{w}>$$

$$\Rightarrow<\mathbf{v},\mathbf{w}>=0, \text{ since } \lambda\neq\lambda_A.$$

For $\overline{\lambda}_A$, the $W_{\overline{\lambda}_A}$ subspace defined by:

$$v_1=0;\cdots;v_{2N+P}=0;\mathbf{t}_1\cdot\begin{pmatrix}v_{2N+P+1}\\v_{2N+P+2}\\\vdots\\v_{2N+2P}\end{pmatrix}=0;\cdots;\mathbf{t}_N\cdot\begin{pmatrix}v_{2N+P+1}\\v_{2N+P+2}\\\vdots\\v_{2N+2P}\end{pmatrix}=0$$

is considered.

In addition to this, we have that:

$$W_{\overline{\lambda}_A}\subseteq E_{\overline{\lambda}_A}{}^C\cap E_{\overline{\lambda}_A}{}^F\cap\overline{E}_{\overline{\lambda}_A}{}^C\cap\overline{E}_{\overline{\lambda}_A}{}^F.$$

being $P-N \le \dim_C(W_{\bar{\lambda}_A}) \le P$.

Lemma 2.- $\bar{\lambda}_A$ is an eigenvalue of **A** and $\dim_C(E_{\bar{\lambda}_A}{}^C \cap E_{\bar{\lambda}_A}{}^F \cap \overline{E}_{\bar{\lambda}_A}{}^C \cap \overline{E}_{\bar{\lambda}_A}{}^F) \ge P-N$.

Proposition 2.- If λ is an eigenvalue of **A**, being $\lambda \neq \lambda_A$, then:

i) The vectors of $E_\lambda{}^C$ are hermitian orthogonal to the vectors of $E_{\bar{\lambda}_A}{}^C \cap \overline{E}_{\bar{\lambda}_A}{}^F$.

ii) The vectors of $E_\lambda{}^F$ are hermitian orthogonal to the vectors of $E_{\bar{\lambda}_A}{}^F \cap \overline{E}_{\bar{\lambda}_A}{}^C$.

The proof of this propositon is analogue to the one in the previous case.

3.2 The decoupling process.

The decoupling consists of a change of the system basis or, more exactly, of the W_{λ_A} subspace eigenvectors. Due to the multiplicity of the λ_A eigenvalue, it is possible to recombine the *P-N* eigenvectors of this subspace obtaining a set of *P-N* linearly independent new vectors, in function of which the mirror inputs and outputs are non-interconnected among them. These eigenvectors correspond to the λ_A eigenvalue, which ensures the system dynamics has not been modified. As a consequence of the change of basis, the system:

$$\dot{\mathbf{x}} = \mathbf{A}*\mathbf{x} + \mathbf{B}*\mathbf{U}_{real}$$
$$\mathbf{Y}_{real} = \mathbf{C}*\mathbf{x}$$

becomes, as a result of a similarity transformation:

$$\dot{\mathbf{z}} = \mathbf{dl}*\mathbf{z} + \mathbf{bn}*\mathbf{U}_{real}$$
$$\mathbf{Y}_{real} = \mathbf{cn}*\mathbf{z}$$

or, in function of the set of non-interconnected inputs and outputs we have called $\mathbf{U}_{virtual}$ and $\mathbf{Y}_{virtual}$, respectively:

$$\dot{\mathbf{z}} = \mathbf{dl}*\mathbf{z} + \mathbf{bv}*\mathbf{U}_{virtual}$$
$$\mathbf{Y}_{virtual} = \mathbf{cv}*\mathbf{z}$$

It has been used the relation between ($\mathbf{U}_{real}$, $\mathbf{Y}_{real}$) and ($\mathbf{U}_{virtual}$, $\mathbf{Y}_{virtual}$), expressed as:

$$\mathbf{U}_{virtual} = \mathbf{T}_u * \mathbf{U}_{real}$$
$$\mathbf{Y}_{real} = \mathbf{T}_y * \mathbf{Y}_{virtual}$$

As it can be seen in figure 2, the 'transformation matrices', T_u and T_y, define the sytem decoupling.

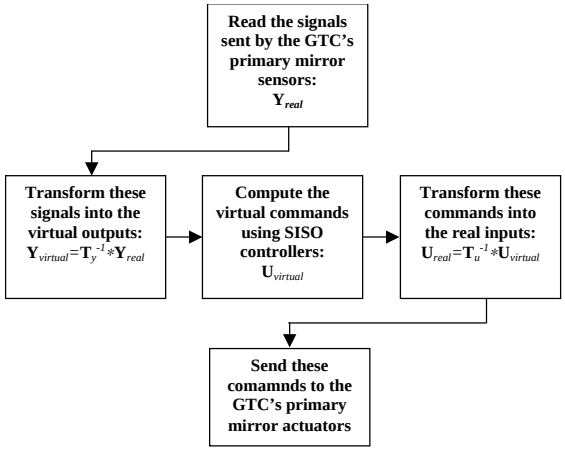

Fig. 2. The control process with the decoupled system.

Simplifying the decoupling method. In the way it was originally proposed (Acosta, 2000), the procedure designed for obtaining the new eigenvectors of the GTC's primary mirror for the system dynamics decoupling presents some aspects that can be improved. Those are:

1. The conditions imposed to the new eigenvectors for ensuring the segments decoupling.
2. The algorithm followed to generate each new eigenvector starting from the W_{λ_A} subspace.

Both can be simplified in such a way that, without losing efficiency:

1. The conditions the new eigenvectors must comply with consist of imposing that the rank of both **b** and **c** matrices of the system once the decoupling is achieved is equal to the number of positioners considered.

2. When imposing the conditions in 1, a linear system of *P-N* equations with 2(*P-N*) unknown quantities is obtained. Thus, *P-N* linearly independent eigenvectors complying with the decoupling conditions can be obtained by simply giving values to the *P-N* parameters of the system of equations.

These two items produce an improvement in the decoupling results. These are even better if the new basis eigenvectors are orthogonalized among them and then normalized in order to minimize the numerical problems that appear when calculating the inverse of the eigenvectors matrix. The decoupling can not be applied when uncertainties in the plant dynamics are considered, since this breaks the λ_A eigenvalue multiplicity. In this case, the T_u and T_y matrices calculated for the nominal plant are used and the decoupling results quickly get worse as uncertainties increase. In spite of this, the closed-loop system with proportional or integral decentraliced SISO controllers is very robust when including these disturbances.

The meaning of the decoupling. Thanks to the decoupling it is possible to transform the original plant into a set of smaller and non-interconnected

subsystems. In fact, one of these has as many inputs and outputs as modes (in general, *N*) are used for the dynamic characterization of the cell that supports the mirror. The rest are SISO subsystems. From the point of view of the segments control, the decoupling plays a fundamental role since reduces the problem of designing a controller for a large-scale multivariable system to the design of a controller whose size will vary in function of *N* and a set of *P-N* SISO ones. Because of this, the decoupling makes the study and application of a great number of control techniques keeping all the information related to the system interconnection possible.

4. A ROBUST CONTROLLER FOR THE DECOUPLED SYSTEM

With the aim of ensuring noise rejection and stability in presence of disturbances, the design of a robust H_∞ controller for the decoupled system has been carried out.

4.1 The control specifications.

The specifications of the control system for the primary mirror of the GTC can be summed up as avoiding that the noise and the multiplicative uncertainties in the model that affect the mirror as shown in figure 3 strains its paraboloidal surface and diminishes the quality of the images it provides. Both performance specifications can be mathematically formulated using the sensitivity *S*(*s*) and the complementary sensitivity *T*(*s*) functions.

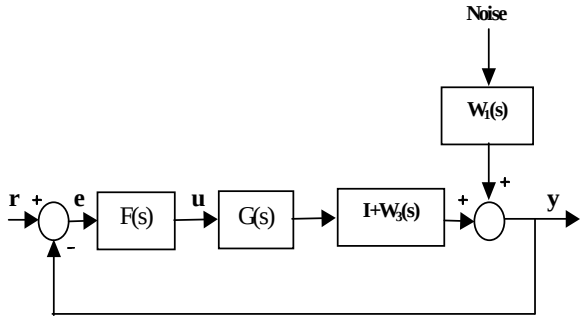

Fig. 3. The closed-loop system weighted model scheme.

As a consequence of the Safonov's theorem (Chiang, 1992), the following inequality is obtained:

$$\bar{\sigma}(T(jw)) \le \left|W_3^{-1}(jw)\right|$$

where $\bar{\sigma}(T(jw))$ is the maximum singular value of the complementary sensitivity function, and $W_3(jw)$ reports on the model uncertainties. This result means that the inverse of the higher multiplicative disturbance is an upper limit to the maximum singular value of the close-loop transfer function *T*(*s*). Moreover, the maximum singular value of the sensitivity function is limited by the inverse of $W_1(jw)$, that gives an account of the noise input:

$$\bar{\sigma}(S(jw)) \le \left|W_1^{-1}(jw)\right|$$

On the one hand, in reference to the noise, the spectrum of its power density is:

$$S(f) = \frac{4/f_0}{\left(1+70.8\left(f/f_0\right)^2\right)^{+5/6}} F^2$$

being f_0=10Hz and F=6N.

With the aim of obtaining a transfer function for the noise, the assumption that it is the output of a linear system whose input is unitary power white noise has been made. Applying that the spectral power density of a random process coincides with its autocorrelation function Fourier transform and approximating the 5/6 exponent in the denominator of *S*(*f*) by the unity for achieving a linear model, a first order transfer function is obtained. It can be proved that the spectrum corresponding to this function and the one of the noise specifications is practically the same.

On the other hand, respect to the uncertainties in the model of the primary mirror, it must be noticed that they are mainly produced by two factors. Those are: 1) a ±5% variability of the segments' base stiffness around its nominal value, which is $6\times10^6\,N/m$, and 2) a random settling time for each positioner after applying a command, which is given by an uniform distribution between 10 and 50ms.

Taking into account the disturbances that affect the primary mirror of the GTC telescope described above, the following curves are obtained:

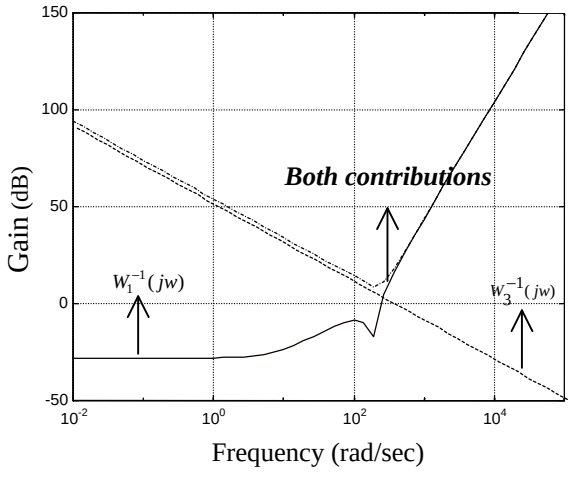

Fig. 4. Disturbances specifications for the robust controller design.

The transfer functions obtained for $W_1^{-1}(s)$ and $W_3^{-1}(s)$ are:

$$W_1^{-1}(s) = \frac{1.8e-7\cdot s^3 + 3.3441e-6\cdot s^2 + 0.006\cdot s + 0.0448}{1.7002}$$

$$W_3^{-1}(s) = \frac{1}{0.002\cdot s}$$

It must be noticed that $W_3^{-1}(s)$ has been approximated by an integral factor. This approximation respects the bandwidth imposed by the uncertainties, which is its most important characteristic from the controller point of view.

5. RESULTS

A robust fifth-order controller for noise rejection has been designed (Zhou, 1998) according to the specifications in figure 4, that report on the disturbances that affect the plant. This is the lowest order controller that produces a good performance from the point of view of noise rejection.

The closed-loop system response with the robust controller designed is shown in figure 5:

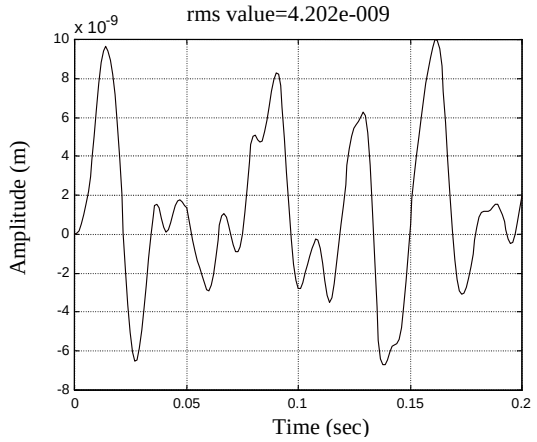

Fig. 5. Closed-loop system response in presence of noise with the SISO robust controller.

The open and closed-loop simulations have been carried out in presence of noise. In addition to this, the positioners time delay varies in a range of 0-5ms, and a ±5% uncertainty in the nominal value of the segments' base stiffness ($6\times10^6 N/m$) has been considered. A noise rejection of, approximately, one order of magnitude is achieved with the controller designed. This result obtained in simulation is tested in the scale model of the GTC's primary mirror consisting in two square iron segments, as shown in figure 6:

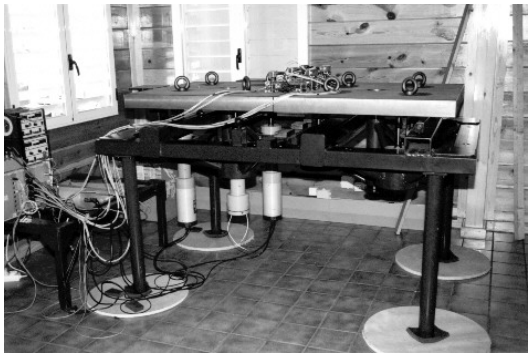

Fig. 6. General view of the GTC's primary mirror scale model.

6. CONCLUSIONS

A series of results related to the design of an active control system for the primary mirror of the Gran Telescopio Canarias have been presented in this paper. Firstly, some properties the system presents and which are used in the mirror dynamics decoupling process are demonstrated. The decoupling has been carried out due to the complexity of designing a centralized controller for a large-scale system whose multiple inputs and outputs are strongly interconnected among them. Then, the general lines of the method of decoupling developed have been exposed. The importance of this procedure, consisting of a change of basis, lies in the fact that it allows to face the control of a multivariable plant without having to neglect any information about the system coupling. Some modifications of the original decoupling procedure whose goal is to simplify and improve it, have been also shown.

A fifth-order robust controller has been designed for noise rejection for any of the subsystems resulting from the decoupling of the GTC's primary mirror dynamics. Considering both noise and uncertainties in the model, a noise rejection of one order of magnitude is achieved.

7. ACKNOWLEDGMENTS

This work has been partially financed by GRAN TELESCOPIO CANARIAS, S.A.

REFERENCES

Acosta L., M. Sigut, A. Hamilton, J. A. Méndez, G. N. Marichal and L. Moreno (2000). Decoupling of the 10m GRANTECAN telescope's primary mirror dynamics and design of a controller for noise rejection. *Proceedings of the 2000 American Control Conference*, June, 2000, Chicago, pp. 2108-2112.

Chiang, R. And M. Safonov (1992). *Robust control toolbox user' guide.*

Hayakawa, K., K. Matsumoto, M. Yamashita, Y. Suzuki, K. Fujimori and H. Kimura (1999). Robust H^∞-Output Feedback Control of Decoupled Automobile Active Suspension Systems. *IEEE Transactions on Automatic Control*, **VOL. 44, NO. 2**, pp. 392-396.

Huang, S. and S. Zhang (1998). Comments on decentralized control for symmetrically interconnected systems. *Automatica*, **VOL. 34, NO. 7**, pp. 929-933.

Skogestad, S. and I. Postlethwaite (1998). *Multivariable feedback control*. John Wiley & Sons. Chichester.

Zhou, K. and J. C. Doyle (1998). *Essentials of robust control*. Prentice-Hall. Englewood Cliffs, NJ.